

# Low Temperature, Shape-selective Formation of Sb<sub>2</sub>Te<sub>3</sub> Nanomaterials and their Thermoelectric Applications

U. Nithiyantham,<sup>§</sup> Sivasankara Rao Ede,<sup>§</sup> M. Fevzi Ozaydin,<sup>#</sup> Hong Liang<sup>#</sup>, A. Rathishkumar<sup>@</sup> and Subrata Kundu<sup>\*§</sup>

<sup>§</sup>Electrochemical Materials Science (ECMS) Division, <sup>@</sup> Central Instrumental Facility (CIF) Division, CSIR-Central Electrochemical Research Institute (CECRI), Karaikudi-630006, Tamil Nadu, INDIA.

<sup>#</sup>Materials Science and Mechanical Engineering, Texas A&M University, College Station, TX 77843-3123, USA.

\* To whom correspondence should be addressed, *E-mail: skundu@cecri.res.in; kundu.subrata@gmail.com*, Phone: (+ 91) 4565-241487, FAX: +91-4565-227651.

## Instruments.

The synthesized Sb<sub>2</sub>Te<sub>3</sub> nanomaterials were characterized with several spectroscopic and microscopic techniques like UV-Vis, TEM, FE-SEM, EDS, XRD, thermal analysis and FT-IR analyses as discussed below. The UV-visible (UV-Vis) absorption spectra were recorded in a double beam UV-Vis spectrophotometer purchased from Unico (model 4802) equipped with a 1 cm quartz cuvette holder for liquid samples. The Transmission Electron Microscopy (TEM) analysis was done with JEOL-JEM 2010 and Tecnai model TEM instrument (TecnaiTM G2 F20, FEI) with an accelerating voltage of 200 KV. The Energy Dispersive X-ray Spectroscopy (EDS) analysis was done with the Field Emission Scanning Electron Microscopy (FE-SEM) instrument with a separate EDS detector connected to that instrument. The FE-SEM study was done with Zeiss ultra FE-SEM instruments. Dried PbTe powder was directly used for the X-ray diffraction (XRD) studies, and Fourier Transform Infrared Spectroscopy (FT-IR) analyses. The XRD analysis was done with a scanning rate of 7°/min in the 2θ range 15-70° using a Bruker X-ray powder diffractometer (XRD) with Cu Kα radiation (λ = 0.154 nm). The thermal analysis study was recorded with a thermal analyser-simultaneous TGA/DTA instrument with model name SDT Q600 and the analysis was performed in air. A hot air oven (temperature up to 250 °C) was used to anneal the samples at specific temperature. The FT-IR analysis was done with the model Nexus 670

(FTIR), Centaurms 10X (Microscope) having spectral Range 4,000 to 400  $\text{cm}^{-1}$  with a MCT-B detector. For TE measurement the sintering process was done by carver press with an Agilent 6680A DC power supply having applied voltage  $\sim 0-5\text{V}$  with a potential of 0-850A. Modulated DSC (MDSC) measurement was done using TA instruments Q2000 modulated DSC with temperature range is  $-180$  to  $725$   $^{\circ}\text{C}$  with accuracy of  $\pm 0.1^{\circ}\text{C}$ .

### **UV-Visible (UV-Vis) spectroscopic study.**

Figure S-1 shows the UV-Vis absorption spectra of the reaction mixtures at different stages of the synthesis process. Curve a is the absorption spectrum of only an aqueous CTAB solution which has no specific absorption band in the UV-Vis region. Curve b is the absorption band of di-ethylene glycolic  $\text{SbCl}_3$  salt solution which also has no specific band as seen in Figure S-1. Curve c is the absorption band of aqueous dispersion solution of Te metal powder which also has no noticeable peak in the UV-Vis region. Aqueous solution 2,7-DHN has three distinct absorption peaks having band maxima at 283, 310 and 324 nm due to the presence of benzenoid chromophores in its structure as seen in curve d in Figure S-1. A mixture of all the reactants like CTAB,  $\text{SbCl}_3$ , Te metal powder, NaOH, 2,7-DHN shows several absorption peaks at 289, 300, 313 and 328 nm (curve e, Figure S-1), similar to the absorption peak of 2,7-DHN. In addition of these peaks, a small hump or a broad peak appeared near 360 nm probably due to absorption of metal salts with CTAB or other interaction among them. After completion of the reaction and centrifugation of the final product, the pure  $\text{Sb}_2\text{Te}_3$  nanomaterials was dispersed in aqueous solutions and sonicated for few min. Curve f and g are the absorption spectra of the two different  $\text{Sb}_2\text{Te}_3$  nanomaterials solution having dumb-bell like, chain-like morphology. We have not seen any specific band or peak for the  $\text{Sb}_2\text{Te}_3$  nanomaterials. As there are no reports of the UV-Vis spectra of  $\text{Sb}_2\text{Te}_3$  nanomaterial, we are unable to compare our electronic spectra with previous literature.

### **EDS analysis.**

Figure S-2 is the result obtained from the energy dispersive X-ray spectroscopic (EDS) analysis which is used to identify the probable elements present in the synthesized product. As representative, we used dumb-bell like morphology for EDS analysis here although other morphology such as chain-like is also measured which gave almost similar spectral feature which is expected. The EDS spectrum consisted of the different peaks for Sb,

Te, C, O, Cl and Br. The large intense Sb and Te peak came from the synthesized  $\text{Sb}_2\text{Te}_3$  nanomaterials. The Cl peak is originated from the chlorinated salt of antimony used during the synthesis. The C, O and Br peaks are come from the CTAB used during the synthesis which acted as a capping agent of our synthesized  $\text{Sb}_2\text{Te}_3$  nanomaterials. Similar types of EDS spectral analyses were reported earlier by Dong et al.<sup>29</sup> and Shi et al.<sup>21</sup> for their synthesis of  $\text{Sb}_2\text{Te}_3$  nanomaterials. Moreover, there was no overlapping EDS spectrum, because all the expected peaks are appeared nicely from the synthesized nanomaterials.

### **Thermal analysis.**

Figure S-3 is the combined thermogravimetric analysis (TGA) and differential thermal analysis (DTA) of the as-synthesized  $\text{Sb}_2\text{Te}_3$  nanomaterials on CTAB micellar media where we used dumb-bell like morphology for entire TGA-DTA analysis. The other chain-like morphology is also tested and gave similar feature (not shown here). From the TGA curve (curve A) we can see that there is no weight loss initially until 400 °C which indicates the absence of any water molecules or moisture in the sample. The first weight loss takes place near 450-470 °C that might be due to the removal of excess surfactant or organic molecules from the sample. After that, another significant weight loss takes place at 586 °C might be due to melting of  $\text{Sb}_2\text{Te}_3$  nanomaterials. After that, another significant weight loss takes place from 819 to 1000 °C. This weight loss after 819 °C is probably due to loss of carbon which is present due to decomposition of CTAB surfactant or other organic molecules. Dong et al. observed the melting point of  $\text{Sb}_2\text{Te}_3$  nanosheets at 417.9 °C which is lower than the reported melting point for bulk  $\text{Sb}_2\text{Te}_3$  nanosheets which is at 620 °C.<sup>28</sup> We started our experiment with 5.82 mg of sample and after heating up to 1000 °C, the amount of sample remained was 3.28 mg which indicates the % of weight loss is 43.6%. On the other hand, from the DTA curve (curve B), there is no noticeable change is observed. A broad exotherm is observed near 354 °C and another at 575 °C is due to the removal of surfactant and melting of  $\text{Sb}_2\text{Te}_3$  nanomaterials. After that, the curve is gradually reduced down and no other exotherm is observed. From the TGA/DTA analysis, we mainly conclude that more weight loss is mainly due to excess or unreacted Te metal powder as it has low melting point compared to Sb or  $\text{Sb}_2\text{Te}_3$ .

Reference 21, 28 and 29 as given here is mentioned under the main text.

The Figures related to UV-Vis study, EDS analysis and TGA-DTA analysis are given below.

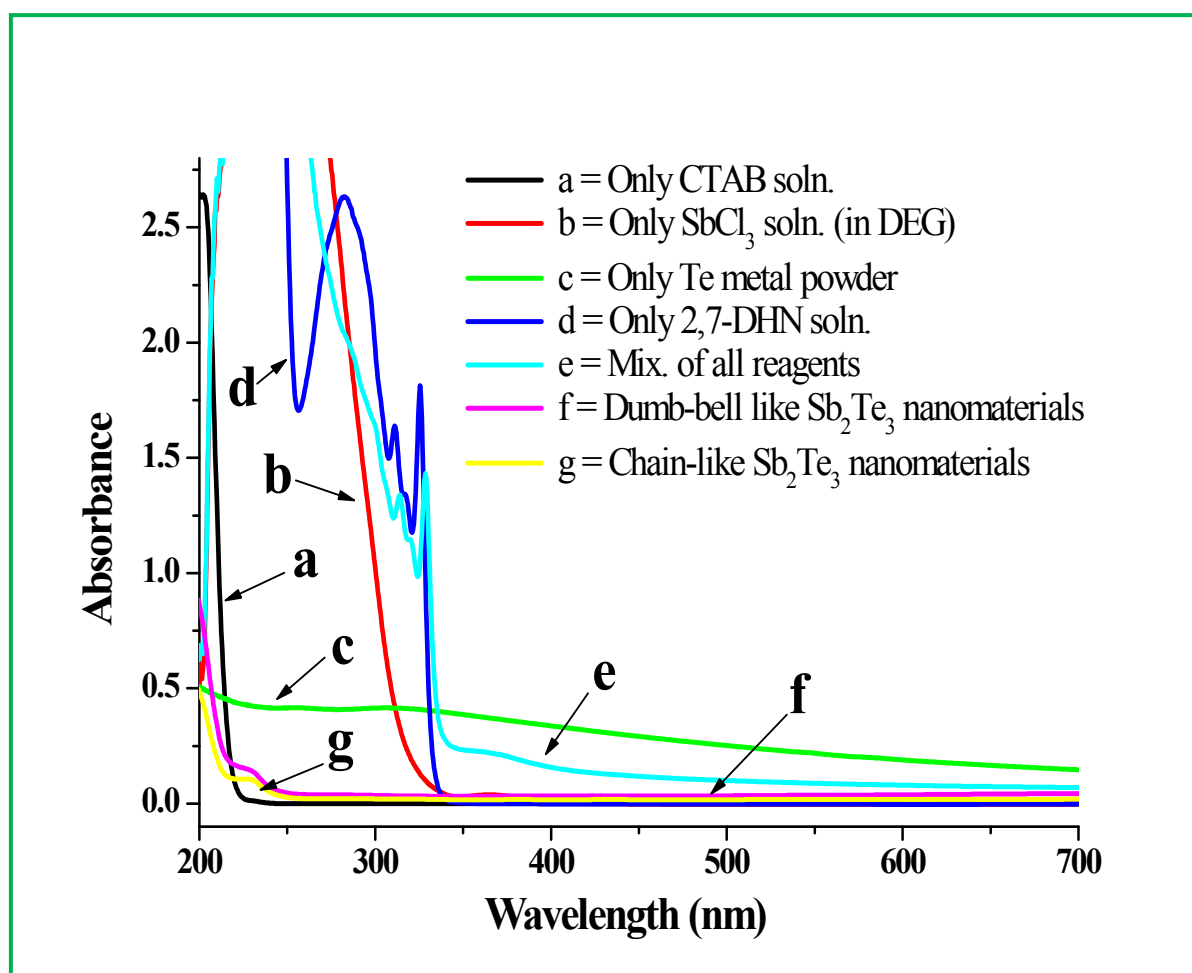


**Figure S-1:** UV-Visible absorption spectra of the reaction mixtures at the different stages of the synthesis process. Curve (a) shows the absorption band of only aqueous CTAB solution; curve (b) shows the absorption band of di-ethylene glycolic SbCl<sub>3</sub> salt solution; curve (c) shows the absorption band of aqueous dispersion solution of Te metal powder; curve (d) shows the absorption band of aqueous dispersion of 2,7-DHN solution; curve (e) shows the absorption band of a mixture of CTAB, SbCl<sub>3</sub>, Te metal powder, NaOH and 2,7-DHN solution; curve (f) and curve (g) shows the absorption band of the two different Sb<sub>2</sub>Te<sub>3</sub> nanomaterials solution having dumb-bell like and chain-like morphology respectively.

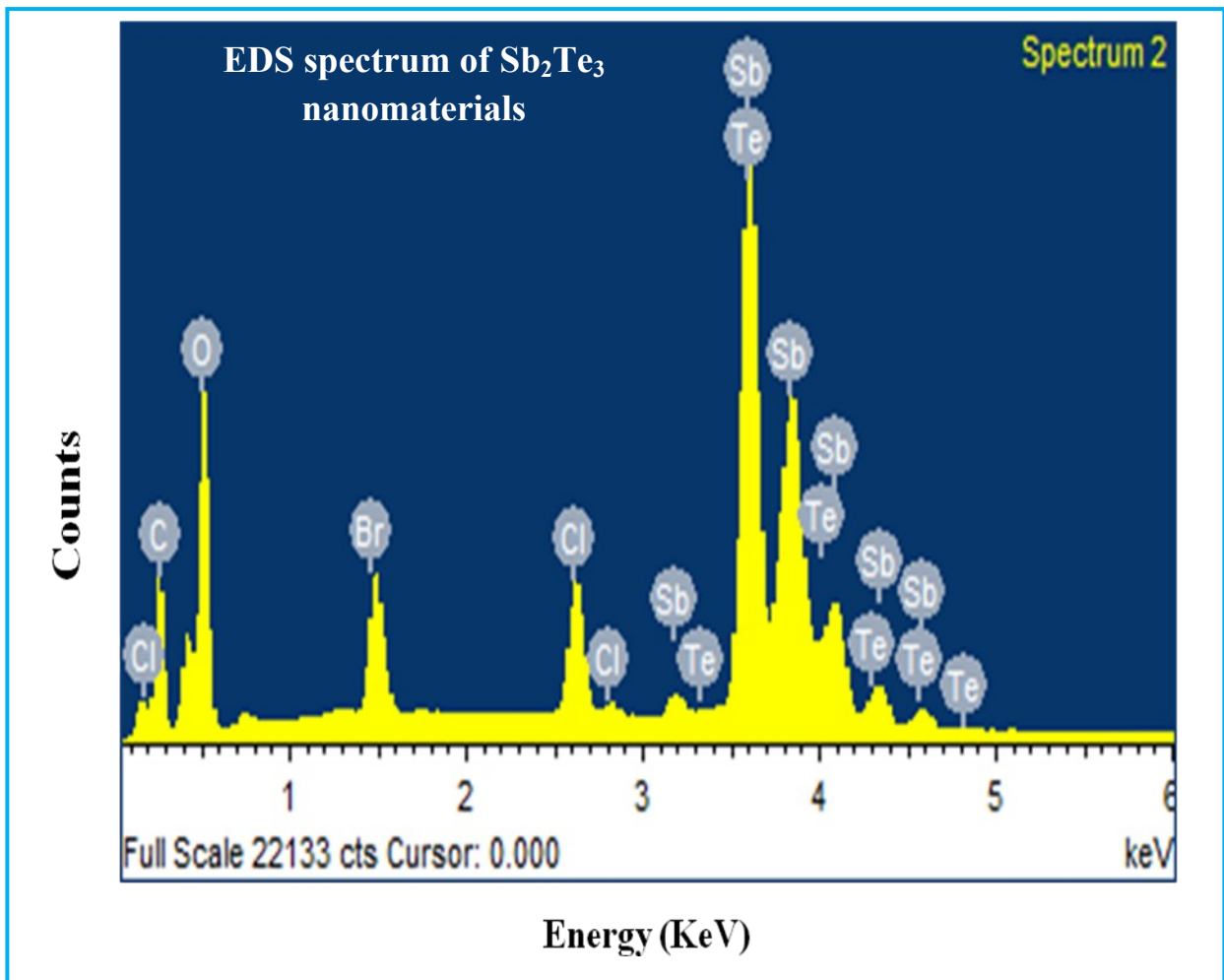


**Figure S-2:** The energy dispersive X-ray spectroscopic (EDS) analysis of Sb<sub>2</sub>Te<sub>3</sub> nanomaterials which consists of the different peaks for Sb, Te, C, O, Cl and Br.

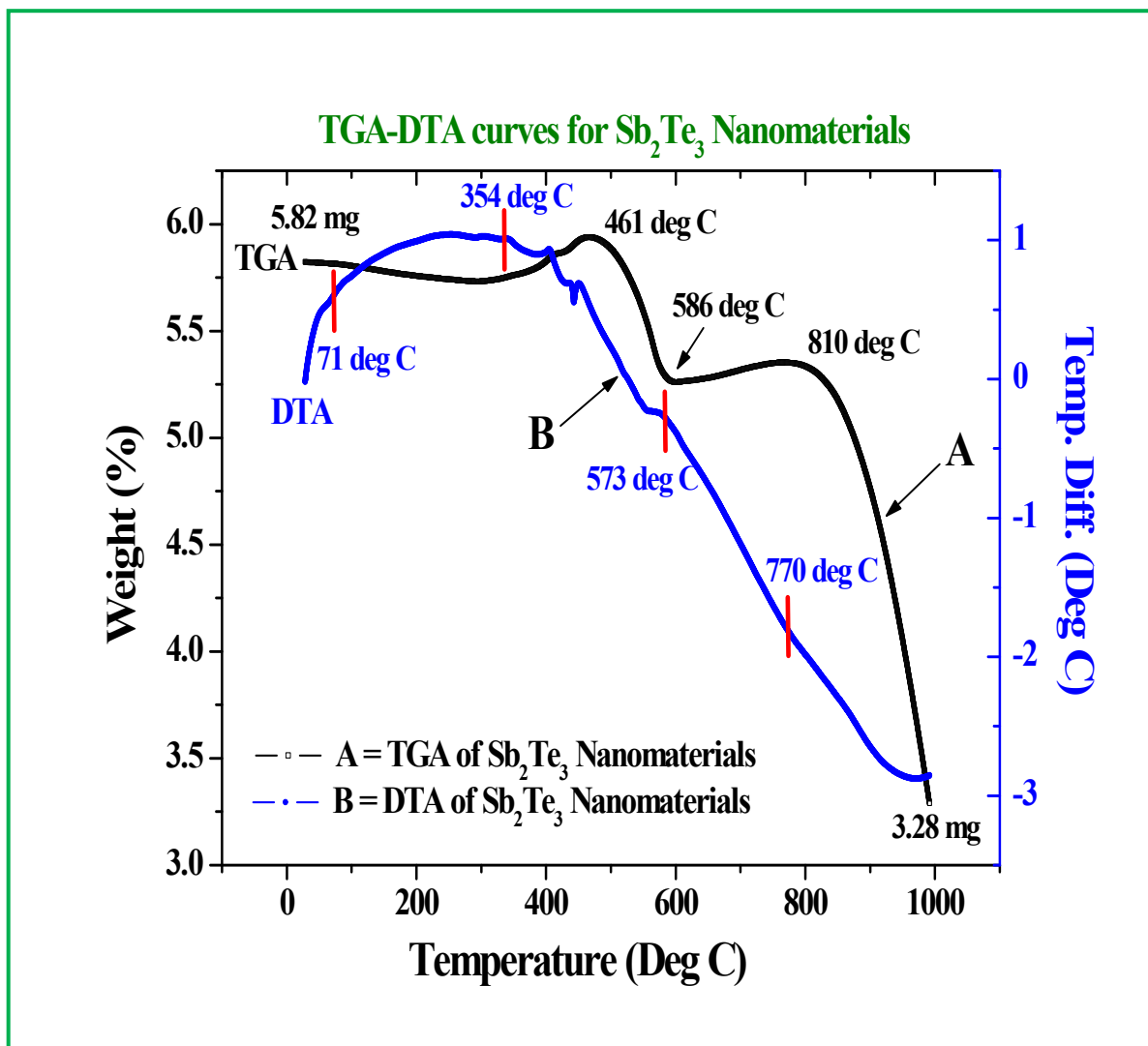


**Figure S-3:** The thermogravimetric analysis (TGA, curve A) and differential thermal analysis (DTA, curve B) of the as-synthesized  $Sb_2Te_3$  nanomaterials on CTAB micellar media.

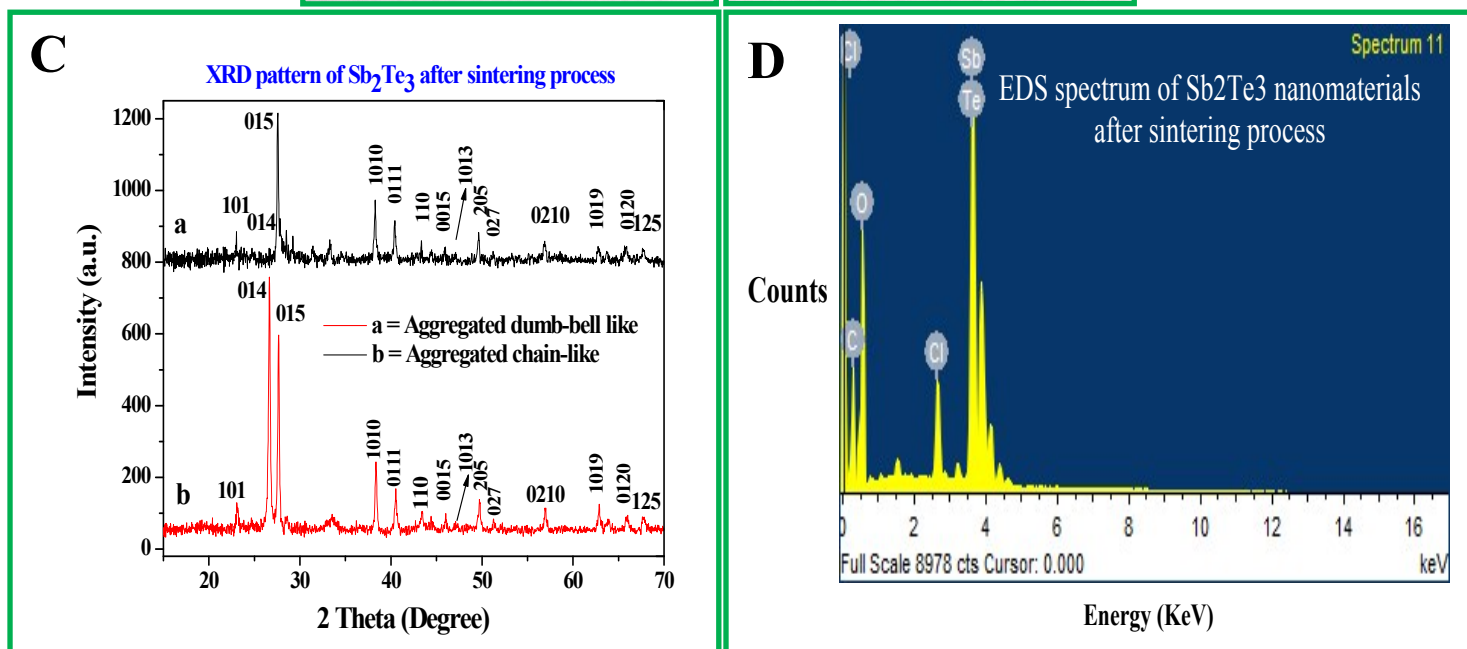
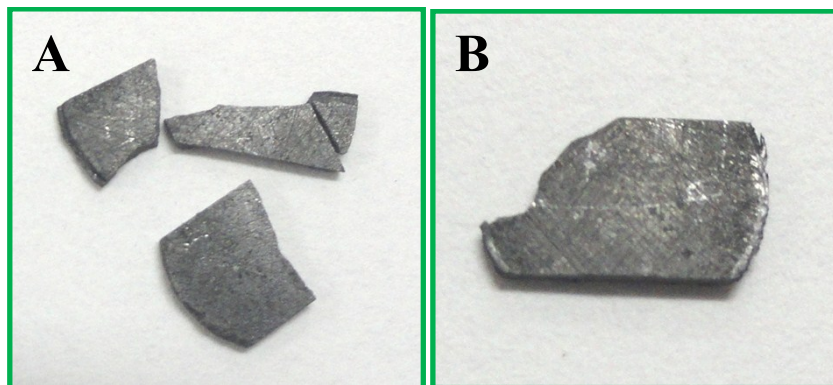


**Figure S-4:** A and B shows the camera images of the  $Sb_2Te_3$  nanomaterials after sintering process. C shows the XRD pattern of the  $Sb_2Te_3$  nanomaterials after sintering process (curve ‘a’ for aggregated dumb-bell like and ‘b’ for aggregated chain-like morphology). D shows the EDS analysis of the aggregated dumb-bell like morphology after sintering process.